University of North Carolina Asheville
Journal of Undergraduate Research
Asheville, North Carolina
December 2021

# Developing Anti-Adhesion Derivatives of N-acetylglucosamine: Synthesis and Structural Analysis

Olivia Pistor
Department of Chemistry
University of North Carolina Asheville
One University Heights
Asheville, NC 28804

Faculty Advisor: Dr. Caitlin McMahon

## Abstract

Antibiotic resistance is a global health threat perpetuated by current antibiotic practices. Antivirulence is a novel method of combating bacterial infections that involves disarming the infection strategies of bacteria without killing them, thereby decreasing selective pressures leading to resistance. Biofilm formation is a virulence factor occurring in roughly sixty-five percent of all microbial infections. Upon adhesion to a host surface, bacteria colonize and begin to form an extracellular matrix that protects the bacteria from immune and drug defenses and makes infections much harder to treat. Anti-adhesion therapy is a method of antivirulence that uses synthetic sugars to prevent adhesion to host cells and thus inhibit biofilm formation. Rising resistance in the common bacteria *Escherichia coli* (*E. coli*) is of particular concern. *E. coli* lectins F17G and GafD bind N-acetyl-ß-D-glucosamine-presenting receptors on the microvilli of epithelial cells causing diarrheal illness, urinary tract infections, and other complications. Adhesion of enterotoxigenic *E.coli* to microvilli can be inhibited by incubation with N-acetylglucosamine, commonly known as GlcNAc. This study works to develop high affinity derivatives of GlcNAc to maximize inhibition of bacterial adhesion, and thereby prevent biofilm formation and reduce bacterial virulence. Inhibitors are synthesized through glycosidation of per-acetylated GlcNAc with various alcohols, followed by deacetylation to remove the protecting groups. Benzyl, hexyl, and phenyl glycosides are successfully developed. Flash column chromatography and nuclear magnetic resonance (NMR) are used for purification and structure determination, respectively. Computational studies with AutoDock Vina and Pymol are performed to assess docking of the GlcNAc derivatives in the receptor protein. The benzyl glycoside is found to have the highest binding affinity, followed by phenyl. The hexyl glycoside does not show a significant improvement to the binding affinity of the natural GlcNAc ligand. This work complements previous research on various E.coli lectins and offers novel insight into F17G binding of GlcNAc derivatives for adhesion inhibition.

## 1. Introduction and Background

Antibiotic resistance is a perpetually growing issue which threatens the population with increasing illness and death due to pathogenic bacteria. In 2014, the World Health Organization (WHO) declared antimicrobial resistance a public health crisis requiring global action. Antibiotics have been exploited by the food industry and over-administered to the effect that common infections such as urinary tract infections and diarrheal illness are becoming resistant to available treatments.[1] Antibiotics are used in food animals to prevent illness and promote growth, however, this practice has been deemed unnecessary and increases the likelihood for resistance to develop. Misuse of antibiotics in healthcare is another contributing factor to rising resistance. According to the Centers for Disease Control (CDC), more than 2.8 million people in the United States alone acquired a drug-resistant bacterial infection in 2019, resulting in at least 35,000 deaths.[2] Infections involving resistant bacteria are detrimental to the U.S. economy and healthcare system as they require longer, more costly treatments, additional doctors' visits, and increase disability and death. Rising resistance in one of the most common pathogenic bacteria, *Escherichia coli*, or *E.coli*, is currently considered

a serious threat by the CDC and is the focus of this study.[2] Enterotoxigenic *E. coli* causes diarrheal illness while uropathogenic *E.coli* is associated with urinary tract infections. Both illnesses are routine and can generally be resolved quickly using standard antibiotics. However, without drastic changes and new strategies for the treatment of microbial infections, previously easy to treat infections such as those related to *E. coli* may soon become life threatening.

Resistance to antibiotics arises as a result of evolution and natural selection. Bacteria possessing a resistance mechanism are not killed by antibiotic treatment and thus continue to grow and multiply, quickly generating a resistant population. The microscopic nature of bacteria lends to large populations and rapid reproduction, so slight variations in genetic information provide enough basis for naturally selected resistance to develop. Additionally, bacteria engage in a phenomenon known as horizontal gene transfer which involves the exchange of genetic material from one organism to another, and even across bacterial species.[3] These characteristics allow bacteria to quickly share favorable genes and rapidly spread resistance throughout a population.[3] Traditional antibacterial strategies perpetuate the cycle of resistance in which, as new drugs are created, bacteria develop new resistance due to the selective pressures induced by antibiotic treatment.[1] Therefore, current antibiotic research and development is ineffective and unsustainable. As first and second tier antibiotics become ineffective, more intense treatments are employed which many be more toxic and harmful to patients and increase associated risks of antibiotic treatment.[2] Furthermore, the use of antibiotics can increase patients' susceptibility to other bacterial and viral infections such as *Clostridium difficile*, or *C.diff*. Infections of *C.diff* bacteria cause life-threatening diarrhea and most frequently occur in hospitalized or recently hospitalized patients.[2] These infections spread quickly because they are resistant to many antibiotic strains and take advantage of the decreased commensal bacteria defense in patients taking antibiotics.[2] The rising threats of antibiotic resistance and futile efforts of current research encourages the development of new strategies to combat bacterial infections. Recently, scientists have gained interest in antibacterial methods which intend to limit the selective pressures leading to resistance by targeting non-essential functions of bacteria rather than those related to growth and viability.

Antivirulence is a novel strategy that has gained popularity in research within the past two decades. The antivirulence approach attempts to disarm the ways bacteria cause infection without killing them, thus decreasing selective pressures contributing to resistance. Bacterial virulence describes the effectiveness of pathogenicity, or how well it interacts with its host and causes infection. Factors of virulence include toxin excretion, efflux pumps, biofilm formation, quorum sensing, and more.[4] While only recently popularized, antivirulence strategies actually pre-date antibiotics. In 1893, Emil von Behring discovered an antiserum which worked against the toxin of diphtheria to decrease pathogenic effects of infection.[3] Yet these findings were quickly shadowed by discovery and successful application of antibiotics.[3] The antivirulence approach is favorable for many reasons, the greatest being the potential to reduce or eliminate the selective pressures leading to resistance by targeting non-essential bacterial functions, while making the infections easier to treat.[3] Additionally, the high specificity for antivirulence targets will be less detrimental to commensal bacteria and overall less harmful to patients. However, experimental testing for resistance has not yet been accomplished in antivirulence research.[1]

Biofilm formation is a virulence factor commonly seen in chronic infections and occurring in roughly 65% of all microbial infections.[5] Bacterial biofilms are comprised of an extracellular matrix of polysaccharides that holds the organisms and fortifies them against immune and drug defense.[5] Biofilms utilize resistance mechanisms such as efflux pumps and antibiotic converting enzymes, making some infections extremely difficult to treat.[4] Biofilm formation occurs as bacteria adhere to a host surface upon which it can colonize (Figure 1).[5] Adhesion occurs via protein-carbohydrate interactions between bacterial lectins and the carbohydrate-coated surfaces of biological host cells.[7] Lectins are carbohydrate-binding proteins found at the tips of the extracellular extensions, pili and fimbriae.[6] Lectins show high specificity for their target carbohydrate ligands, leading to adherence at specific locations and tissue types.[6] While only a small number of bacterial lectins have been characterized, the potential for each bacterium to express numerous different adhesin types is recognized, as this ensures adhesion imperative to infection and biofilm development.[8] Interactions between the natural sugars and their respective lectins generally show low affinities in the millimolar range.[7] Biochemical investigations have improved affinity by several orders of magnitude using synthetic derivatization of the natural sugar ligands.[7] This opens the door for a new anti-biofilm strategy involving inhibition of adhesion with synthetic carbohydrate ligands. Research within the past two decades has demonstrated the ability for exogenous carbohydrates to block bacterial adhesion to animal cells in vitro, and mono- and polyvalent saccharides have successfully protected mice, rabbits, calves, and monkeys from infection by lectin-presenting bacteria.[7]

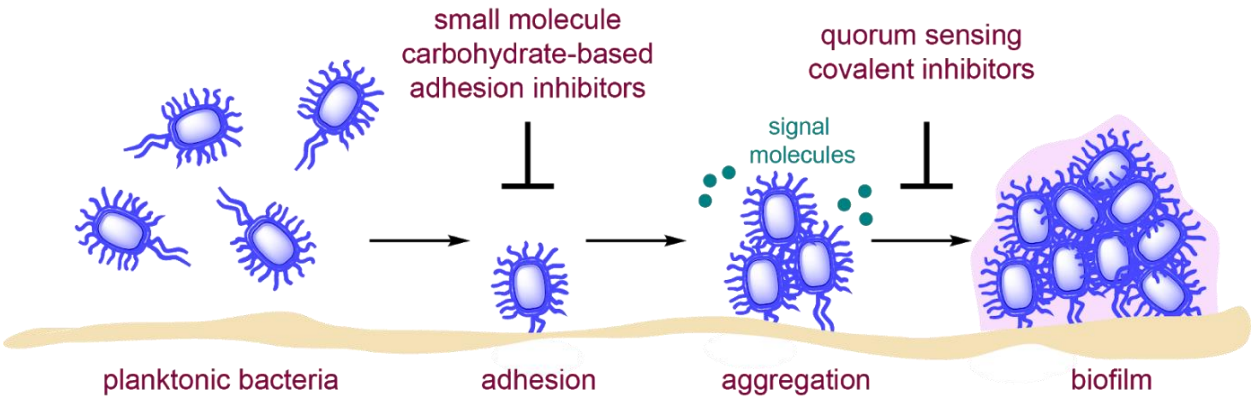


Figure 1. Biofilm formation process - preventing adhesion halts biofilm formation. (McMahon)

Blocking the initial adhesion step is a method of antivirulence first reported in 1955 by Collier and Miranda, who found successful inhibition of *E. coli* adhesion with mannose.[6] Mannose-binding type 1 pili are important virulence factors of uropathogenic *E.coli* and are among the most well-characterized bacterial lectins.[9] Crystallographic analyses of the FimH receptor binding domain in a study by Bouckaert and colleagues revealed the structure and stability of the lectin domain, as well as important residues involved in binding.[9] This study also found variable affinity measurements for mannose, common mono- and disaccharides, and several aryl and alkyl mannosides, and reported increased affinity for simple alkyl mannosides.[9] Many studies have shown improved affinity with hydrophobic substitutions on the mannose sugar, with aromatic α-mannosides found to be potent inhibitors of type 1 fimbriated *E.coli*.[7] This is likely due to the presence of a hydrophobic region next to the extended binding site identified through X-ray crystallography.[7] X-ray studies have also revealed binding site interactions with all of the hydroxyl groups except for the anomeric position, making this position favorable for substitution to improve affinity.[7]

However, there are multiple expressible fimbrial adhesins for enterotoxigenic and urotoxigenic *E.coli* strains.[8] Despite showing no significant sequence homology, *E.coli* lectins GafD and PapG have similar characteristsics and are thought to be related to FimH through divergent evolution.[10] The lectins all share a beta-barrel jelly-roll fold of the protein and bind their respective lectins on the side of the protein, but display differences in their ligand binding domains.[10] The presence of a secondary binding domain has been identified in FimH and GafD, but was previously considered irrelevant due to very low affinity binding interactions with the natural ligands.[10] However, a 2010 study by T.K. Lindhorst and colleagues attempted FimH inhibition with a bivalent glycopeptide consisting of two mannose glycosides connected by a linker designed to bridge two binding sites.[11] Unfortunately the bivalent ligand did not show significantly improved inhibition compared to a simple methyl-mannopyranoside and did not prove to occupy two sites. This may be due to improper size, conformation, or entropy issues, and should be investigated further since bacteria are known to bind host cells multivalently.[11] Likewise, increased affinity was demonstrated in attachment to polymeric carriers to form multivalent ligands. [7,12] A review published by Imberty et. al. summarized the findings that multivalent ligands generally show much higher affinities for bacterial lectins and show strong potential for inhibition in topical infections.[13] However, these inhibitors were not applicable to systemic infections and were limited by low oral bioavailability.[4]

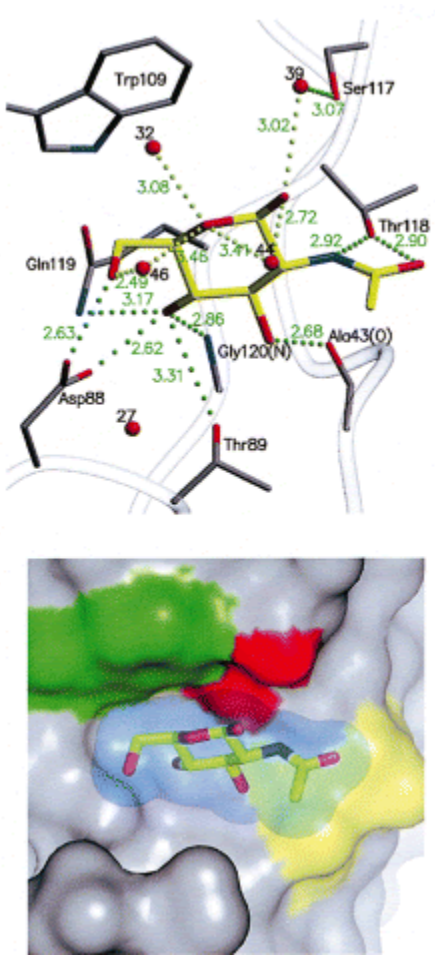


Figure 2. F17G protein complexed with GlcNAc.[14] Binding residues shown (top), protein surface shown (bottom).

The FimH, F17G, and PapGII fimbrial adhesins all display an immunoglobin-like fold of the lectin structural components which encapsulate the ligand.[14] While some functional redundancy has been recognized in vitro, variation in adhesins contributes to binding specificity and aids in persistence of adhesion despite shear conditions in vivo.[8] Ligand specificity differs among bacterial strains and infections and is determined by the amino acid residues present in the binding site.[10] Therefore, a more comprehensive understanding of bacterial adhesion via various adhesin proteins is needed to advance the anti-adhesion approach of antivirulence. F17G and GafD are lesser studied adhesive lectins of *E.coli.* F17G is involved primarily in bovine infections, while GafD is more relevant in human infections.[10] The lectins have been found to play important roles in adhesion as well as fimbrial biogenesis and are therefore important targets in anti-adhesion therapy.[15] The F17G/GafD lectin binds to N-acetyl-ß-D-glucosamine-presenting receptors on the microvilli of intestinal epithelial cells, causing diarrheal illness.[14] Adhesion of enterotoxigenic *E.coli* to microvilli can be inhibited by incubation with N-acetylglucosamine (GlcNAc) or GlcNAc oligomers.[15] Investigation of the lectin domain by university research groups in Brussels and Stockholm revealed a shallow, elongated shape formed by the carbonyl of Ala43 and the side chains of residues Asp88, Thr89, Trp109, Ser116, Thr117, Gln119, and the nitrogen of Gly120. These residues were conserved across five *E. coli* variants.[15] The pocket is approximately 329 Å and could accommodate an additional monosaccharide.[10] Specificity for GlcNAc appears to occur around Thr117-Asn44, where Thr117 positions the amide through hydrogen bonding (Figure 2). Furthermore, the Trp109 residue forms a hydrophobic contact with the sugar moiety where the indole ring is parallel with the sugar ring.[10] Figure 2 illustrates the F17G protein complexed with the GlcNAc ligand.

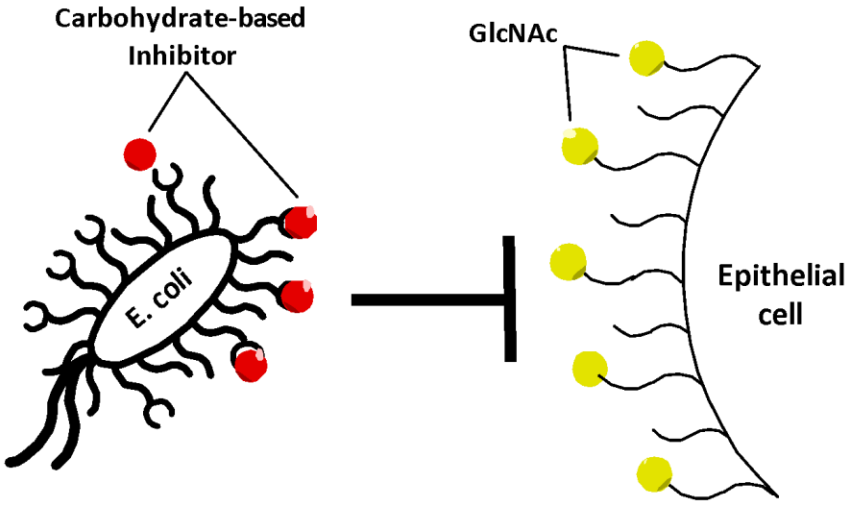


Figure 3. Inhibition of E.coli adhesion with GlcNAc-based inhibitors

The low affinity trend among lectins for their natural carbohydrate ligands is consistent in the F17G-GlcNAc interaction, allowing for improvement through synthetic derivation of GlcNAc.[9] This project aims to design and synthesize carbohydrate-based inhibitors of the F17G and GafD adhesins to prevent adhesion and biofilm formation by *E.coli* bacteria (Figure 3). Beginning with a protected GlcNAc glycosyl acceptor, glycosidation with various alcohols followed by deprotection will generate a library of potential inhibitors (Scheme 1, Figure 4). Crystallographic analysis of the F17G protein indicated a broad hydrophobic region adjacent to the binding site.[14] Therefore, alkyl extensions at C1 may induce greater affinity through hydrophobic interactions and shielding, lending to decreased entropy. Computational docking studies with Autodock and Pymol provide the relative binding affinities and highlight important binding interactions among the GlcNAc derivatives. In future work, the affinity of the potential inhibitors will be assessed using ELISA-like assays. *E. coli* will be cultured to test the synthetic ligands' adhesion and biofilm inhibition abilities using hemagglutination and crystal violet assays. Additionally, cell growth and death will be assessed to ensure success in disarming without killing the bacteria. The protein-ligand complexes will be crystallized and analyzed to provide insight of binding interactions and guide subsequent syntheses. This work hopes to develop the first effective inhibitors of F17G/GafD and elucidate useful information for the development of anti-adhesion therapy to combat bacterial infections.

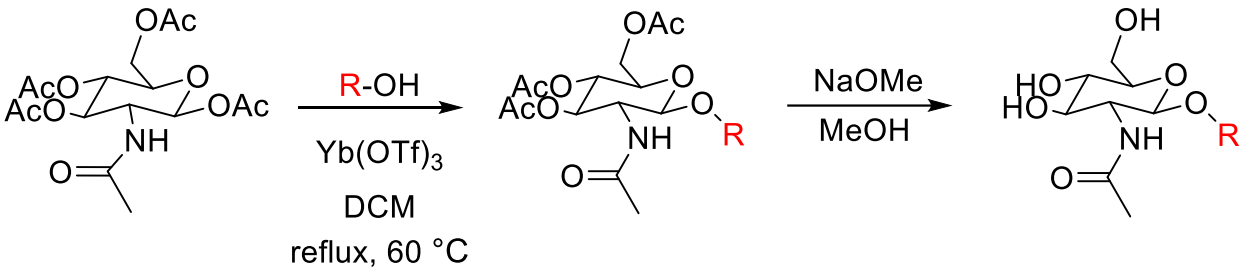


Scheme 1. General synthesis plan for GlcNAc glycosidation

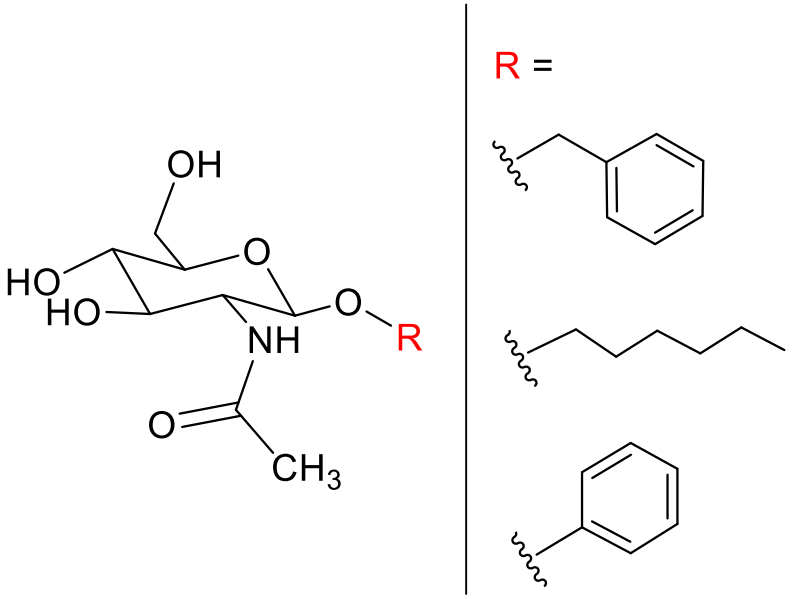


Figure 4. Potential derivations of GlcNAc

## 2. Experimental

### 2.1 General Methods

Chemical reagents were purchased from Alfa Aesar. Anhydrous solvents were dried over molecular sieves in the solvent system. Reaction progress was monitored using thin layer chromatography (TLC) on SiliaPlates and visualized with UV and potassium permanganate stain ($KMnO_4$), unless otherwise noted. Reactions were concentrated under reduced pressure using a Heidolph rotary evaporator. Purification was achieved using flash chromatography on columns of silica ($SiO_2$ 40-63 μm, 230-400 mesh). Product characterization was accomplished through proton nuclear magnetic resonance ($^1$H NMR) spectroscopy. Analysis was performed on a 400 MHz Varian spectrometer with solvent resonance as the internal standard ($CDCl_3$ at 7.27 ppm). $^1$H NMR data are reported as follows: chemical shift, multiplicity (s = singlet, d = doublet, t = triplet, q = quartet, quin = quintet, sxt = sextet, dd = doublet of doublets, ddd = doublet of doublet of doublets, dt = doublet of triplets, td = triplet of doublets, qd = quartet of doublets, m = multiplet, br. s. = broad singlet), coupling constants (Hz), integration, and proton identifier.

### 2.2 Synthesis of 2-acetamido-3,4,6-triacetyl-2-deoxy-α-D-glucopyranosyl chloride (**0**)

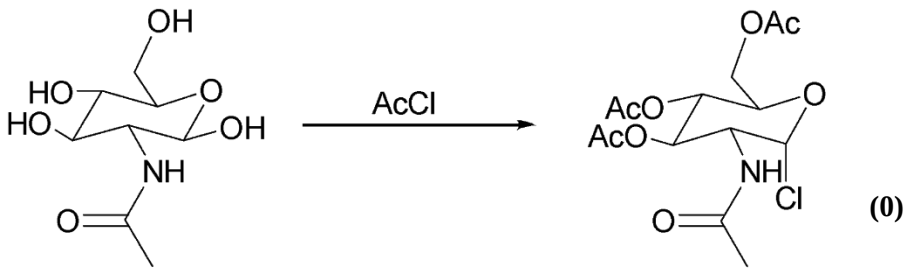


**(0)**

Scheme 2. Synthesis of peracetylated GlcNAc chloride (**1**) for use as starting material

The protected glycosyl acceptor **1** was synthesized according to the procedure put forth by Horton (Scheme 2).[16] N-acetylglucosamine was dried at 25 °C with under vacuum for 6 hours prior to use. In a round bottom flask equipped

with a reflux condenser and protected with a tube of calcium sulfate, acetyl chloride (9 eq., 210 mmol, 10 mL) was added to N-acetylglucosamine (1 eq., 22.6 mmol, 5.0 g) over 2-3 minutes. Additional acetyl chloride (4.4 eq., 100 mmol, 5 mL) was added to achieve a stirrable mixture, and the reaction stirred for 72 hours at room temperature. Chloroform ($CHCl_3$, 22 eq., 50 mmol, 40 mL) was added through the condenser before the solution was poured with vigorous stirring over ice (40 g) and water (10 mL) in a clean beaker. The reaction was extracted and drawn off into a new beaker containing ice and saturated sodium bicarbonate solution (40 mL). Neutralization was completed in a clean separatory funnel and the reaction was extracted into a flask containing anhydrous magnesium sulfate ($MgSO_4$, 250 mg). The extraction and neutralization process must be completed quickly, in less than 15 minutes, as the product reacts rapidly with water especially while acidic. The reaction was stirred for 10 minutes before the $MgSO_4$ was removed by Büchner funnel and washed with dry DCM. The reaction was concentrated by rotary evaporation at 50 °C. Ether, dried overnight with 4 Å molecular sieves, was added to the warm solution and the reaction was left to crystallize overnight. The product was collected onto a Büchner funnel, well washed with dry ether and allowed to dry on the vacuum for 5 minutes to yield a light-tan solid (5.38 g, 67.7%) $^1$H NMR analysis in $CDCl_3$ confirmed the product but showed evidence of an off-target product as well.

## 2.3 Synthesis of Benzyl 2-acetamido-2-deoxy-ß-D-glucopyranoside (**2**) from GlcNAc Chloride

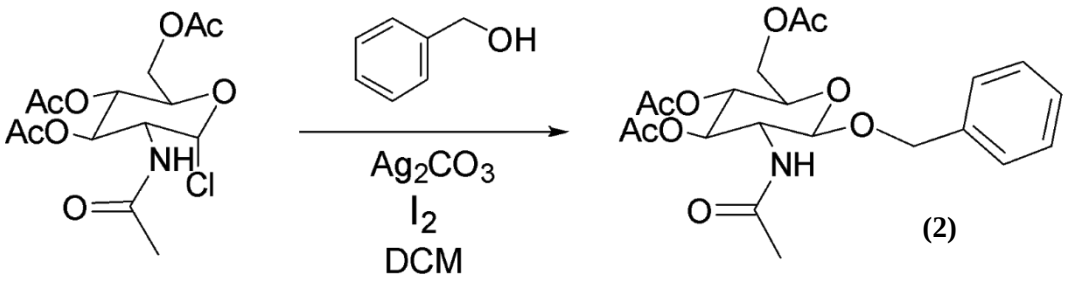


Scheme 3. Glycosidation of GlcNAc chloride with benzyl alcohol

The glycosidation of per-acetylated GlcNAc chloride with benzyl alcohol was carried out according to a published procedure (Scheme 3).[17] This procedure was first attempted with commercial starting material purchased from Chem-Impex and re-attempted with the chloride prepared in-house (Scheme 2). The reaction was carried out in an inert argon atmosphere and the reaction flask was covered with aluminum foil. Silver carbonate (3 eq., 0.73 mmol, 201.0 mg), benzyl alcohol (5 eq., 1.2 mmol, 0.12 mL) and a catalytic crystal of iodine were combined and stirred in dichloromethane (DCM, 14, 3.48 mmol, 0.222 mL) over 4 Å molecular sieves for 15 minutes. Simultaneously, the acetylated sugar (1, 0.24 mmol, 85.1 mg) was stirred in dry DCM (0.222 mL) over 4 Å molecular sieves. The sugar solution was added dropwise to the reagents and the reaction was left to stir for 21 hours. Once TLC indicated completion, the reaction was diluted with ethyl acetate, filtered through glass wool and Celite and concentrated under reduced pressure. The product was purified by column (20% EtOAc/Hexane), and fractions showing product spotting in TLC were combined and concentrated. Analysis of both glycosidation attempts with the chloride showed inconclusive results. $^1$H NMR in $CDCl_3$ indicated excess ethyl acetate and hexane, but peaks for the intended product could not be confirmed.

## 2.4 Synthesis of Benzyl 2-acetamido-2-deoxy-α-D-glucopyranoside (**2**)

### *2.4.1 Benzyl 2-amino-3,4,6-tri-O-acetyl-2-deoxy-β-d-glucopyranoside (**1**)*

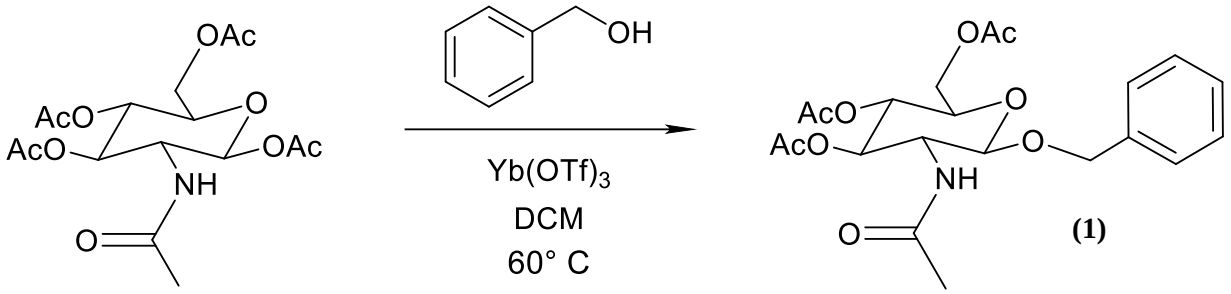


Scheme 4. Glycosidation of ß-D-glucosamine pentaacetate with benzyl alcohol

The synthesis of the benzyl glycoside (**2**) was accomplished in two steps according to a procedure from Shultz et. al, beginning with ß-D-glucosamine pentaacetate as the protected glycosyl acceptor.[18] The reaction was conducted under an inert atmosphere of argon in a 60 ºC oil bath. Beta-D-glucosamine pentaacetate (1 eq., 0.624, 0.25 g) was added to a dry, 10 mL round bottom flask. Dry dichloromethane (5 mL), ytterbium triflate (0.12 eq., 0.077 mmol, 0.0478 g) and benzyl alcohol (3 eq., 1.92 mmol, 0.2 mL) were added sequentially to the flask and the reaction was stirred with reflux for 23 hours. The reaction was removed from the oil bath and allowed to cool to room temperature before being washed three times with deionized water, dried with $MgSO_4$, and concentrated under reduced pressure. Purification by column (5 % hexanes/EtOAc) gave the pure product **1** as a white solid (0.1293 g, 46.05%). Peaks from $^1$H NMR analysis were consistent with the values reported in the literature.[19] $^1$H NMR ($CDCl_3$): δ 7.33-7.38 (m, 5H, Ph), 5.30 (d, *J* = 9.2 Hz, 1H, NH), 5.20, (dd, *J* = 9.6, 9.6 Hz, 1H, H-3), 5.08 (t, *J* = 9.2 Hz, 1H, H-4), 4.89 (d, *J* = 12 Hz, 1H, $CH_2$Ph), 4.63 (d, *J* = 8 Hz, 1H, H-1) 4.62 (d, *J* = 12.4 Hz, 1H, $CH_2$Ph), 4.31 (dd, *J* = 4.8, 4.8 Hz, 1H, H-6a), 4.19 (dd, *J* = 2.8, 2.4 Hz, 1H, H-6b), 3.99 (m, 1H, H-2), 3.68 (m, 1H, H-5), 2.12 (s, 3H, NHAc), 2.03 (s, 6H, 2$COCH_3$), 1.92 (s, 3H, $COCH_3$).

### *2.4.2. Benzyl 2-acetamido-2-deoxy-α-D-glucopyranoside (**2**)*

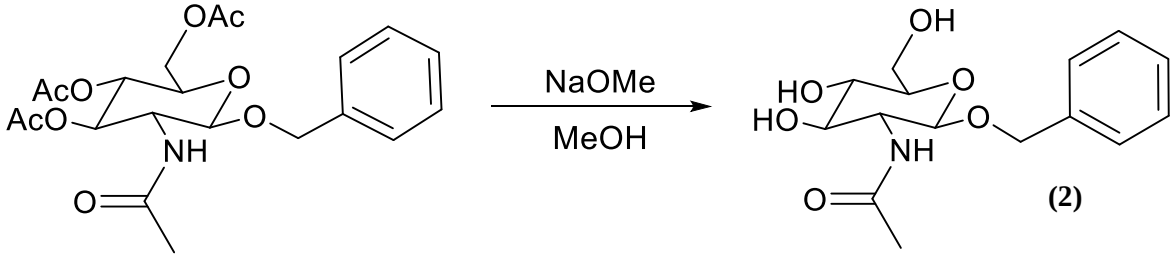


Scheme 5. Zemplen deacetylation of the protected benzyl glycoside

Deacetylation of **1** followed the general Zemplen procedure as reported by Shultz et. al.[18] However, the deprotection methodology was first reported by Zemplen and Kuntz in 1924.[20] In a dry flask, **1** (1 eq., 0.114 mmol, 0.05 g) was combined with anhydrous methanol (1.42 mL). Sodium methoxide solution was diluted from 5.4 M to 0.5 M with anhydrous methanol before being added to the flask (3 eq., 0.342 mmol, 2.1 mL). The solution stirred at room temperature for three hours. Amberlite cation exchange resin was rinsed with HCl followed by D.I. water before being stirred in the solution for 15 minutes and filtered off. The solution was concentrated under reduced pressure to yield the crude product **2** as a light orange-pink solid. The structure was confirmed by $^1$H NMR in $D_2O$ with comparison to the reported literature values.[21] $^1$H NMR ($D_2O$): δ 7.4-7.3 (m, 5H, Ph), 4.8 (d, 1H, $CH_2$Ph), 4.6 (d, 1H, $CH_2$Ph), 4.4 (d, 1H, H-1), 3.9 (dd, 1H, H-6a), 3.8-3.6 (m, 2H, H-6b, H-2), 3.4 (m, 3H, H-3, H-4, H-5), 1.9 (s, 3H, $NHCOCH_3$). Purification was attempted but unsuccessful.

## 2.5 Synthesis of Hexyl 2-acetamido-2-deoxy-β-D-glucopyranoside (**4**)

### 2.5.1 *Hexyl-2-acetamido-3,4,6-tri-O-acetyl-2-deoxy-β-D-glucopyranoside (**3**)*

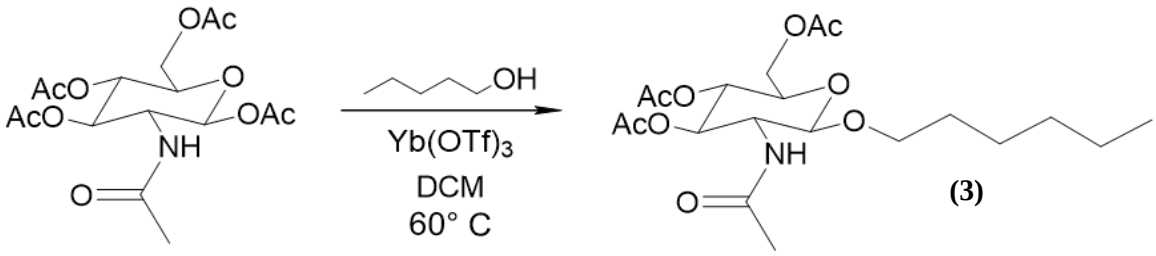


Scheme 6. Glycosidation of ß-D-glucosamine pentaacetate with hexanol

The glycosidation procedure adapted from Shultz et. al was carried out with hexanol to prepare the hexyl glycoside.[18] Under an inert argon atmosphere, ß-D-glucosamine pentaacetate (1 eq., 0.64 mmol, 0.25g), dry DCM (5 mL), ytterbium triflate (0.1 eq., 0.075 mmol, 0.05g), and hexanol (2.6 eq., 1.67 mmol, 0.21 mL) were added sequentially to a dry flask and refluxed overnight in a 60 ºC oil bath. The reaction was extracted in a vial with three portions of deionized water and dried through a pipette column of magnesium sulfate. The product was purified via column chromatography (20 % hexanes/EtOAc) to afford **3** as a white solid (0.12 g, 43.5 %). Analysis was consistent with values reported in the literature.[22] $^1$H NMR ($CDCl_3$): δ 5.46 (d, *J* = 8.4 Hz, 1H, NH), 5.3 (dd, *J* = 8.8, 9.2 Hz, 1H, H-3), 5.10 (t, *J* = 9.6, 9.6 Hz, 1H, H-4), 4.70 (d, *J* = 8.8 Hz, 1H, H-1), 4.29 (dd, *J* = 5.2, 4.4 Hz, 1H, H-6a), 4.5 (dd, *J* = 2.4, 2.4 Hz, 1H, H-6b), 3.88 (m, 2H, H-2, $OCH_2$), 3.7 (m, 1H, H-5), 3.45 (m, 1H, $OCH_2$), 2.1, 2.05, 1.9 (s, 12H, $3COCH_3$), 1.30 (br s, 8H, $OCH_2(CH_2)_4$), 0.9 (t, *J* = 6.8, 7.2 Hz, 3H, $OCH_2(CH_2)_4CH_3$).

### *2.5.2. Hexyl 2-(acetamido)-2-deoxy-β-D-glucopyranoside (**4**)*

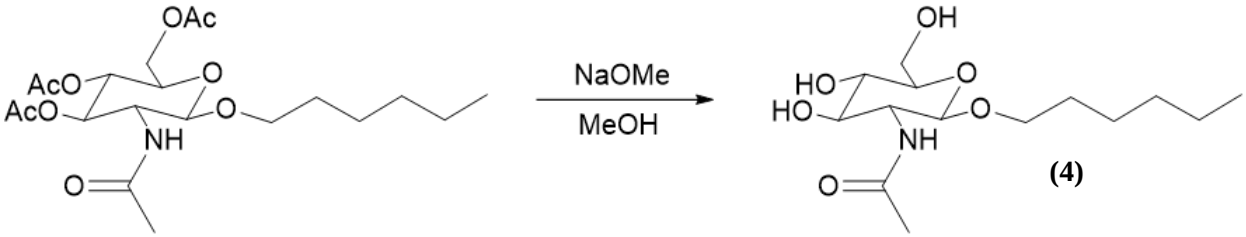


Scheme 7. Zemplen deacetylation of the protected hexyl glycoside

Deacetylation of **3** was accomplished by the previously described procedure.[18] Under an inert atmosphere of argon, 4 (1 eq., 0.185 mmol, 0.08 g) and MeOH (1 eq., 0.184 mmol, 2.3 mL) were combined. NaOMe (3 eq., 0.555 mmol, 1.1 mL) was added and the reaction stirred for two hours. Amberlite exchange resin was rinsed thoroughly with hydrochloric acid and water before being stirred in the reaction for 15 minutes and then removed by filtration. The solution was concentrated to yield a white solid (0.053 g, 66.4%). Purification was carried out by column chromatography (10% MeOH/DCM) and structure analysis confirmed the product according to values reported in the literature.[18] $^1$H NMR ($CD_3OD$): δ 4.32 (d, *J* = 8.4 Hz, 1H, H-1), 3.91-3.22 (m, 8H, H-2, H-3, H-4, H-5, H-6, $OCH_2$), 1.9 (s, 3H, $NHCOCH_3$), 1.5, 1.3 (br m, 8H, $OCH_2(CH_2)_4$), 0.8 (t, *J* = 7.2, 6.8, 3H, $O(CH_2)_5CH_3$).

## 2.6 Synthesis of phenyl 2-acetamido-3,4,6-tri-O-acetyl-2-deoxy-β-D-glucopyranoside (**5**)

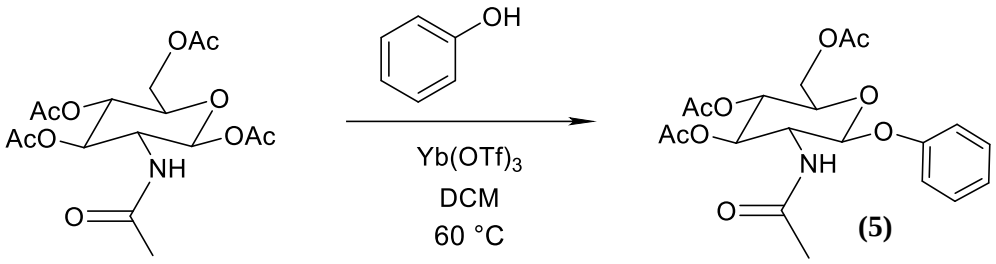


Synthesis of the phenyl glycoside was carried out according to the procedure adapted from Shultz et. al.[18] ß-D-glucosamine pentaacetate (1 eq., 0.64 mmol, 0.25g), dry DCM (122 eq., 78.3 mmol, 5 mL), ytterbium triflate (0.1 eq., 0.075 mmol, 0.05g), and phenol (3 eq., 1.926 mmol, 0.181 g) were combined in a flask under an inert argon atmosphere and refluxed overnight (26 hours) in a 60 ºC oil bath. Excess DCM (5 mL) was added to reconstitute the reaction before extracting with three portions of deionized water. The organic layer was run through a pipette column of magnesium sulfate to dry following the third extraction. The product was purified with column chromatography (5% hexane/EtOAc) to give the protected glycoside **5** as a white solid (0.0741 g, 27.26%). Characterization confirmed the structure with comparison to values reported in the literature.[23] $^1$H NMR ($CDCl_3$): δ 7.29, 7.10 (m, 5H, Ph), 5.57 (d, J = 9.2 Hz, 1H, NH), 5.42 (dd, J = 8.8, 9.2 Hz, 1H, H-3), 5.28 (d, J = 8.4 Hz, 1H, H-1), 5.18 (t, J = 9.6, 9.6 Hz, 1H, H-4), 4.32 (dd, J = 5.2, 5.6 Hz, 1H, H-6a), 4.18 (m, 2H, H-6b, H-2), 3.88 (m, 1H, H-5), 2.08, 2.06, 2.05, 1.97 (s, 12H, $NHOCH_3$, $O(OCH_3)$).

## 2.6 Computational Docking

Molecular modeling and visualization software Autodock Vina and Pymol were used for computational docking of F17G with GlcNAc derivatives. A docking procedure was adapted from Forli et. al. and used in combination with guidance from the Steed Lab to carry out computational studies on the benzyl, phenyl, and hexyl glycosides as well as the natural GlcNAc ligand.[24]

1. Grid box coordinates and dimensions set in AutoDock

| Dimension | Number of points | Center coordinate | Offset |
|---|---|---|---|
| X | 50 | -0.918 | 17.861 |
| Y | 40 | -3.215 | -1.389 |
| Z | 40 | 15.392 | -1.222 |

### *2.6.1 General Docking Procedure*

Protein coordinates for the F17G receptor were taken from the Protein Databank entry 2bsb published by Buts et. al., and prepared in Pymol.[14] The sugar ligand was extracted from the protein and non-bonded molecules, such as water, were removed. GlcNAc analogs were constructed using the ChemDraw suite. The ligand was prepared in AutoDock by detecting the torsion root, adjusting rotatable bonds, and writing the ligand output file. For each of these studies, the amide bond was set to be rotatable. Hydrogens are implicit in the prepared ligand but must be added to the receptor molecule once it is loaded into AutoDock. The ligand coordinates are read into the program and the grid box is centered on the receptor binding site. Grid box coordinates were consistent across each docking and are available in the

supplementary materials. The docking output files were visualized in Pymol. Polar contacts were identified using a preset ligand site mode with labeled residues. Hydrogen bond interactions were assumed where contact between a hydrogen and oxygen atom was indicated.

## 3. Docking Results

Computational docking studies were successfully carried out for the benzyl, hexyl, and phenyl glycosides. The important binding residues identified were consistent with the literature and include Ala43, Asn44, Asp88, Thr89, Ser116, Thr117, Gln118, and Gly119. In many poses, Trp109 is positioned for potential π stacking, but this has yet to be confirmed in this study. Hydrogen bonds are identified as well as main and side chain polar contacts.

### *3.1 Benzyl 2-acetamido-2-deoxy-α-D-glucopyranoside Docking*

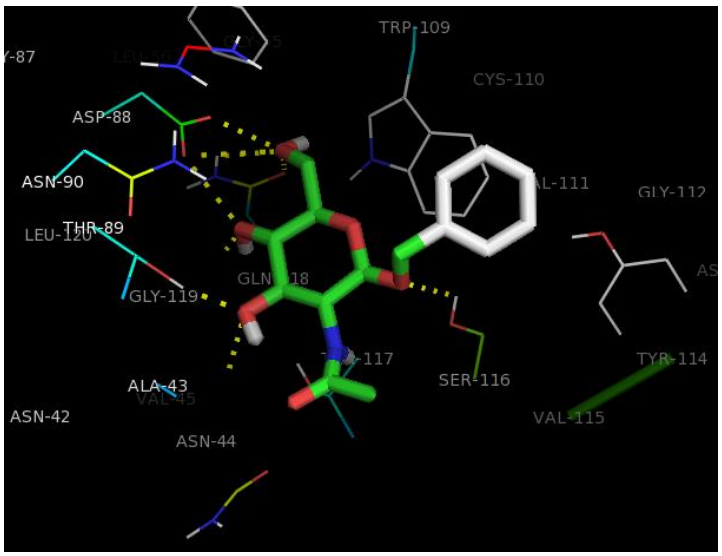


Figure 4. Pose one of benzyl glycoside docked in F17G with polar contacts highlighted.

Table 1. Output of F17G docking of benzyl 2-acetamido-2-deoxy-α-D-glucopyranoside

| Pose | Affinity (kcal/mol) | RMSD l.b. | RMSD u.b. |
|---|---|---|---|
| 1 | -6.7 | 0.000 | 0.000 |
| 2 | -6.5 | 2.035 | 4.744 |
| 3 | -6.3 | 2.318 | 4.343 |
| 4 | -6.1 | 1.451 | 2.120 |
| 5 | -5.9 | 1.844 | 2.634 |
| 6 | -5.9 | 2.123 | 4.432 |
| 7 | -5.7 | 1.190 | 1.633 |
| 8 | -5.7 | 3.738 | 5.579 |
| 9 | -5.7 | 2.769 | 4.898 |

Table 2. Polar Contacts of benzyl 2-acetamido-2-deoxy-α-D-glucopyranoside docking. Hydrogen bonds are indicated by (H) and bidentate interactions by (B). Main chain interactions are denoted by (M).

| Pose | C1-OBn | NH | $OCH_3$ | C3-OH | C4-OH | C6-OH |
|---|---|---|---|---|---|---|
| 1 | Ser116 (H) | Thr117 (H) | -- | Asn44 (M)<br>Thr89 (H) | Asp88<br>Gly119 (M) | Asp88 (B)<br>Gln118 (H, B) |
| 2 | Ser116 (H) | -- | Ala43 (M)<br>Thr89 (H)<br>Gly119 (M) | Ala43 (M) | -- | -- |
| 3 | -- | -- | -- | Asp88<br>Gln118 | Asp88<br>Gly119 (M) | Ala43 (M)<br>Thr117 (H)(M)<br>Gly119 (M) |

Docking of the benzyl glycoside in the F17G receptor protein produced the greatest affinity measurements ranging from -6.7 kcal/mol for the best pose and -5.7 kcal/mol for the seventh, eighth, and ninth poses (Table 1). The benzyl glycoside forms polar contacts in the binding site with each of the oxygen atoms except the amide carbonyl in the highest affinity pose (Table 2). A total of four hydrogen bond interactions are seen in pose one between the benzyl oxygen and Ser116, the amide and Thr117, the hydroxyl of carbon three and Thr89, and the hydroxyl of carbon six and Gln118. Main chain polar contacts are made between carbons three and four with residues Asn44 and Gly119, respectively. Ser116 also hydrogen bonds the benzyl oxygen in pose two, while carbons four and six show no polar interactions. However, the amide oxygen engages in three polar interactions including a hydrogen bond to Thr89 and two main chain interactions around residues Ala43 and Gly119. The oxygen of carbon three also makes a polar contact to the main chain of Ala43. The benzyl oxygen and amide are not engaged in the third pose, yet carbons three, four, and six are multiply engaged. Asp88 interacts with carbons three and four and the main chain of Gly119 contacts carbons four and six. Carbon six hydrogen bonds to Thr117 and makes an additional main chain interaction. Polar contacts for pose one are illustrated in figure 5.

### *3.2 Hexyl 2-acetamido-2-deoxy-α-D-glucopyranoside Docking*

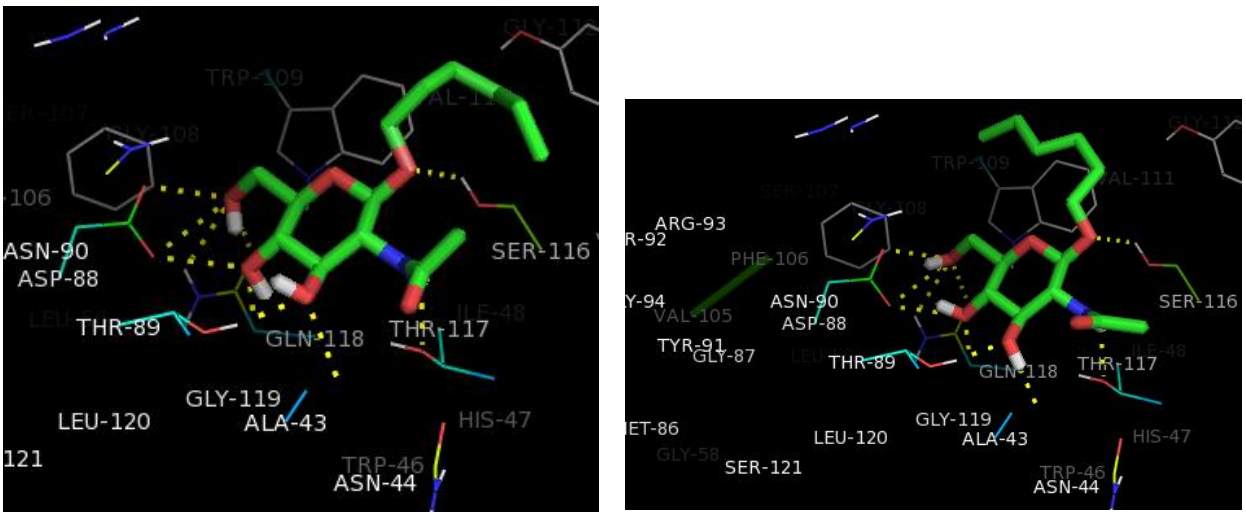


Figure 6. F17G binding residues complexed with the hexyl glycoside in pose one (left) and pose two (right).

Docking the hexyl derivative of GlcNAc gave affinity measurements ranging from -5.8 kcal/mol in the first pose and -4.9 kcal/mol in the ninth pose (Table 3). The first two poses make the same set of polar interactions and have similar orientation of the sugar molecule (Figure 6). They differ only in the position of the alkyl chain and hydroxyls of carbons three, four, and six, which bend in opposite directions between the poses. In total, six hydrogen bonds are made between the hexyl glycoside and the binding residues in the first two poses. Ser116 hydrogen bonds the oxygen

of carbon one while the amide hydrogen binds Thr117. Carbons four and six hydrogen bond Asp88 in pose one while pose two shows only polar interactions between the oxygens. Carbon six makes two bidentate interactions with Asp88 and Gln118 in both poses. Pose three engages the amide oxygen with Asp88, Gln118, and a main chain interaction with Gly119. Main chain polar contacts are also made between Ala43 and carbons three and four, Gly119 and carbon three, and Thr117 with carbon six. Additionally, Asn44 contacts carbons three and four. No hydrogen bonding is observed in the third pose.

Table 3. Output of F17G docking of hexyl 2-acetamido-2-deoxy-α-D-glucopyranoside

| Pose | Affinity (kcal/mol) | RMSD l.b. | RMSD u.b. |
|---|---|---|---|
| 1 | -5.8 | 0.000 | 0.000 |
| 2 | -5.6 | 1.437 | 2.691 |
| 3 | -5.6 | 1.576 | 4.252 |
| 4 | -5.3 | 1.802 | 2.549 |
| 5 | -5.3 | 2.077 | 4.451 |
| 6 | -5.2 | 2.157 | 4.809 |
| 7 | -5.2 | 2.449 | 4.724 |
| 8 | -5.1 | 1.979 | 4.838 |
| 9 | -4.9 | 2.560 | 3.235 |

Table 4. Polar Contacts of hexyl 2-acetamido-2-deoxy-α-D-glucopyranoside docking. Hydrogen bonds are indicated by (H) and bidentate interactions by (B). Main chain interactions are denoted by (M).

| Pose | C1-O$(CH_2)_5CH_3$ | NH | $OCH_3$ | C3-OH | C4-OH | C6-OH |
|---|---|---|---|---|---|---|
| 1 | Ser116 (H) | Thr117 (H) | -- | Ala43<br>Thr89 (H) | Asp88 (H)<br>Gly119 | Asp88 (H, B)<br>Gln118 (H)(B) |
| 2 | Ser116 (H) | Thr117 (H) | -- | Ala43<br>Thr89 (H) | Asp88<br>Gly119 | Asp88 (B)<br>Gln118 (H)(B) |
| 3 | -- | -- | Asp88<br>Gln118<br>Gly119 (M) | Ala43 (M)<br>Asn44<br>Gly119 (M) | Ala43 (M)<br>Asn44 | Thr117 (M) |

*3.2 Phenyl 2-acetamido-2-deoxy-α-D-glucopyranoside Docking*

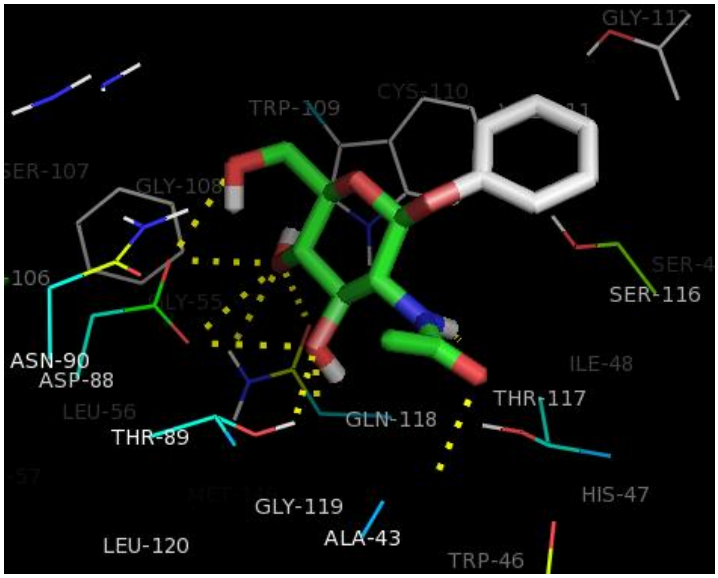


Figure 7. Pose one of phenyl glycoside docked in F17G with polar contacts highlighted.

The phenyl glycoside docking study produced poses with affinity measurements ranging from -6.3 and -6.2 kcal/mol for the top two poses down to -5.2 kcal/mol for the ninth pose (Table 5). The first two poses show no interactions with the phenyl oxygen while the third pose with an affinity of -5.7 kcal/mol shows a hydrogen bond to Ser116 (Table 6). Hydrogen bonding is seen between the amide and Thr117 in the first three poses. Asp88 interacts with carbons four and six in the first three poses, and additionally with carbon three in pose one (Figure 7). Carbon three contacts the main chain of Gly119 in pose one and two while the main chain of Asn44 makes contact in poses two and three. Thr117 makes a main chain contact and hydrogen bond with carbon two in pose two. The amide oxygen is involved in distinct polar interactions in each of the first three poses.

Table 5. Output of F17G docking of phenyl 2-acetamido-2-deoxy-α-D-glucopyranoside

| Pose | Affinity (kcal/mol) | RMSD l.b. | RMSD u.b. |
|---|---|---|---|
| 1 | -6.3 | 0.000 | 0.000 |
| 2 | -6.2 | 1.908 | 2.381 |
| 3 | -5.7 | 1.764 | 2.548 |
| 4 | -5.7 | 1.949 | 4.578 |
| 5 | -5.4 | 2.505 | 4.209 |
| 6 | -5.3 | 1.947 | 3.295 |
| 7 | -5.3 | 3.039 | 4.806 |
| 8 | -5.3 | 2.093 | 4.314 |
| 9 | -5.2 | 2.115 | 4.606 |

Table 6. Polar contacts of phenyl 2-acetamido-2-deoxy-α-D-glucopyranoside docking. Hydrogen bonds are indicated by (H) and bidentate interactions by (B). Main chain interactions are noted as (M).

| Pose | C1-OPh | NH | $OCH_3$ | C3-OH | C4-OH | C6-OH |
|---|---|---|---|---|---|---|
| 1 | -- | Thr117 (H, M) | Ala43 (M) | Asp88<br>Thr89 (H)<br>Gly119 (M) | Asp88 (B)<br>Gln118(H)(B) | Asp88 |
| 2 | -- | Ser116 (H)<br>Thr117 (H, M) | Thr117(M) | Asn44 (M)<br>Thr117 (M) (H)<br>Gly119 (M) | Asp88 (B) | Asp88 |
| 3 | Ser116 (H) | Thr117 (H) | Asn44 | Asn44 (M)<br>Thr89 (H) | Asp88<br>Gly119 (M) | Asp88 (B)<br>Gln118<br>(H)(B) |

## *2.6.5 F17G docking of N-acetylglucosamine*

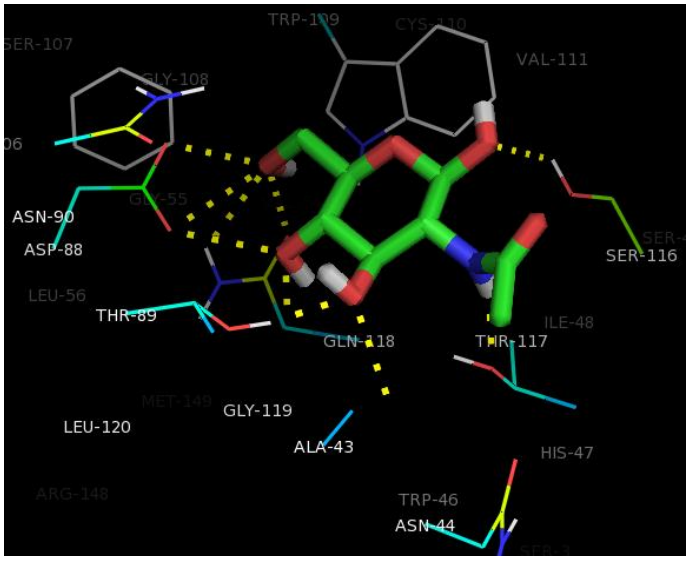


Figure 8. Polar interactions of GlcNAc docked in F17G

Docking of the natural GlcNAc ligand gave an affinity value of -5.7 kcal/mol for the top pose and -4.5 kcal/mol for the ninth pose. In pose one, hydrogen bonding between the amide and Thr117 positions the ligand for hydrogen bonding with the hydroxyls of C3, C4, and C6 deeper in the binding pocket (Figure 8). Poses 2 and 3 gave equal affinity values of -5.3 kcal/mol, yet pose three makes two less polar contacts than pose two (Table 8). Pose two hydrogen bonds through the amide nitrogen while pose three makes polar contacts between the amide oxygen, Asp88 and Gly119. Poses that do not hydrogen bond through the C1 hydroxyl make more polar contacts with the C3 and C4 hydroxyls due to the shifted position.

Table 7. Output of F17G docking with GlcNAc ligand

| Pose | Affinity (kcal/mol) | RMSD l.b. | RMSD u.b. |
|---|---|---|---|
| 1 | -5.7 | 0.000 | 0.000 |
| 2 | -5.3 | 2.567 | 5.152 |
| 3 | -5.3 | 1.923 | 4.958 |
| 4 | -5.1 | 1.989 | 2.248 |
| 5 | -4.9 | 2.238 | 4.904 |
| 6 | -4.7 | 1.639 | 2.913 |
| 7 | -4.6 | 2.763 | 5.640 |
| 8 | -4.6 | 3.016 | 5.672 |
| 9 | -4.5 | 1.656 | 1.819 |

Table 8. Polar binding interactions of GlcNAc with F17G receptor protein

| Pose | C1-OH | NH | $OCH_3$ | C3-OH | C4-OH | C6-OH |
|---|---|---|---|---|---|---|
| 1 | Ser116 (H) | Thr117 (H) | -- | Ala43 (M)<br>Thr89 (H) | Asp88<br>Gly119 (M) | Asp88 (B)<br>Gln118 (H, B) |
| 2 | -- | Asp88 (H) | -- | Trp109 (H)<br>Thr117 (M)<br>Gln118 (H) | Ala43 (M)<br>Thr89 (H)<br>Thr117 (M)<br>Gly119 (M) | Ala43 (M) |
| 3 | -- | -- | Asp88<br>Gln118 | Ala43 (M)<br>Gly119 (M) | Ala43 (M)<br>Thr117 (H) | Thr117 (M) |

## 4. Discussion

### 4.1 Syntheses with GlcNAc Chloride

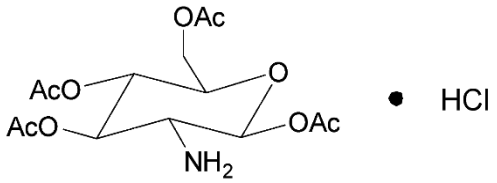


Figure 9. 1,3,4,6-tetra-O-acetyl-2-amino-deoxy-α-D-glucopyranose hydrochloride.

Synthesis of the chloride starting material (Scheme 1) was attempted after glycosidation of commercial starting material with benzyl alcohol was unsuccessful (Scheme 2). The procedure was carried out according to the plan set forth by Horton.[16] The reaction is highly sensitive, especially while acidic, and quickly undergoes acetal transfer to 1,3,4,6-tetra-*O*-acetyl-2-amino-deoxy-α-D-glucopyranose hydrochloride upon exposure to water or moist air (Figure 9).[16] $^1$H NMR analysis of **1** in chloroform showed a doublet of triplets around δ 5.2, indicating the presence of the off-target product. It is noted that the product will degrade quickly if impure.[16] The synthesis of **1** was somewhat successful, but after being stored in a dessicator for five months the product likely degraded and was not suitable for use, leading to inconclusive results in the second glycosidation attempt with benzyl alcohol. $^1$H NMR analysis of the commercial starting material showed the same characteristic peaks and was insoluble in chloroform, indicating impurity. Therefore, due to lack of viable starting material, the chloride procedure was abandoned and new methods involving a different protected glycosyl acceptor were investigated.

## 4.2 Syntheses with GlcNAc Pentaacetate

Several preparation methods for 2-acetamido-2-deoxy glycosides are reported by Beau et. al.[24] A procedure using GlcNAc pentaactetate as the protected glycosyl acceptor with ytterbium triflate as a Lewis acid activator was chosen for its high selectivity of ß-glycosides and good yields. Glycosidations with benzyl alcohol, hexanol, and phenol were accomplished with this method to produce acetylated alkyl glycosides. A similar glycosidation procedure involving scandium triflate is also available and may provide greater kinetic efficiency and higher yields, but this has not been attempted in this study.[24] Deprotection of the benzyl and hexyl glycosides was attempted, yet purification of the resulting GlcNAc derivatives proved to be challenging.

### *4.2.1 Benzyl Glycosidation (**2**)*

The synthesis of benzyl 2-acetamido-2-deoxy-α-D-glucopyranoside (**2**) provided the desired product in decent yield (46.1%). This improves on previous yields where recrystallization was used for purification. Column chromatography appears to be a more efficient method for purification of the glycosides thus far. Yields may be improved during the extraction process by using a suitably sized separatory funnel rather than extracting by pipette in a vial. Crystals formed in the aqueous layers after extraction indicated the possibility of lost product. Additionally, during the overnight reflux the reaction congealed to a viscous jelly that was unable to stir. The addition of excess DCM during the reaction run could improve reaction efficacy by maintaining the correct viscosity.

The deacetylation reaction was attempted twice and produced the benzyl glycoside in low yield (21.7% crude) upon the second attempt. Obtaining a suitable solvent system for purification was challenging and purification was not carried out for the latest deprotected benzyl product. Characterization by NMR was convoluted due to solubility issues with the product, which should be soluble in methanol. In many cases, the Amberlite ion exchange resin likely contaminated the product and left it with an orange tint. Additional laboratory complications during the deprotection procedure contributed to low yield and prevented further investigation of the deprotected benzyl glycoside. However, it does appear to have been successfully synthesized. The deprotected glycoside was marked by a downfield shift of peaks in the spectra and reduction of acetate peaks from three to one. $^1$H NMR analysis of **2** suggests two rotamers of the amide in solution, but this is not of concern in this study.

### *4.2.2 Hexyl Glycosidation (**4**)*

Synthesis of hexyl 2-(acetamido)-2-deoxy-β-D-glucopyranoside (**4**) was successfully completed after two attempts. In the first attempt, the reaction stirred with reflux for the recommended three hours and recrystallization was used for purification. Crystals appeared over time in the filtrate, so these were added to the previously harvested crystals and the product, **3** was concentrated to give the product in low yield (10.4%). It is likely that **3** is slightly soluble in hexanes due to the extended alkyl substituent. Therefore, recrystallization with methanol and hexanes is not suitable for purification of this product. $^1$H NMR analysis of the first attempt showed presence of the starting materials and little evidence of the product, suggesting that the reaction did not run to completion. Yield was improved in the second attempted by allowing the reaction to reflux overnight and was purifying by column chromatography to give the product in good yield (43.5%). Yields may be increased by improving extraction and transfer techniques. $^1$H NMR analysis of **3** after purification of the second attempt gave a pure spectrum with little evidence of leftover reagents.

Deacetylation to afford the hexyl glycoside **4** was carried out successfully with a 71.4% crude yield. Purification by column gave the pure product in 66% yield. Allowing the reaction to run for longer than two hours may improve the pure yield. Rinsing the Amberlite resin with HCl prior to use eliminated the amber coloring previously seen in the benzyl product.

### *4.2.3 Phenyl Glycosidation (**5**)*

Glycosidation of per-acetylated GlcNAc with phenol was successful on the second attempt and produced the protected glycoside **5** in good yield (66.4%). A malfunction with the hot plate led to very little product, as evidenced by the NMR spectra which showed mostly starting material. The second attempt ran to completion to produce a yellow, viscous material that was purified by column to a white solid. The NMR spectra of the purified product shows excess

aromatic peaks and an undesignated cluster around 4.1 ppm. This may indicate an off-target product with a similar polarity to the intended product, that was not fully separated by column. The spectrum also shows a large water peak which may be due to contamination during extraction or concentration by Rotovap. The glycosides developed in this study were synthesized on a small scale and usually concentrated under reduced pressure in a vial. This creates a higher risk for water contamination than standard glassware compatible with the Rotovap. Deacetylation has not yet been attempted on the phenyl glycoside.

## 4.3 Computational Docking

The computational docking studies offer valuable information on the relative affinities for binding of each proposed GlcNAc derivative. The benzyl glycoside appears to be the most promising derivative with the highest affinity binding. The seventh, eighth, and ninth poses of the benzyl glycoside show affinities of -5.7 kcal/mol, equal to the affinity value for the best binding pose of the natural ligand GlcNAc (Table 1). The -6.8 kcal/mol affinity measurement for the top benzyl glycoside pose is a substantial improvement to the GlcNAc binding affinity of -5.7 kcal/mol and greater than either of the other two studied glycosides. This may be due to the benzyl group's ability to extend across the hydrophobic region adjacent to the binding site as previously identified in x-ray crystallography studies.[14] According to the hydrophobic effect, greater shielded surface area of the protein leads to decreased entropy upon binding, which is favorable and leads to a higher affinity binding reaction. Comparatively, the phenyl substituent does not extend as far over the adjacent hydrophobic region and this may explain the differences in affinity between the benzyl and phenyl glycosides. This concept is illustrated in figure 10, yet further analysis of solvent shielding is needed to make definitive observations. Furthermore, the aromatic substituent of the phenyl and benzyl glycosides can potentially align with the Trp109 residue, allowing for favorable π-stacking interactions. However, this remains speculatory until more comprehensive analysis can be achieved.

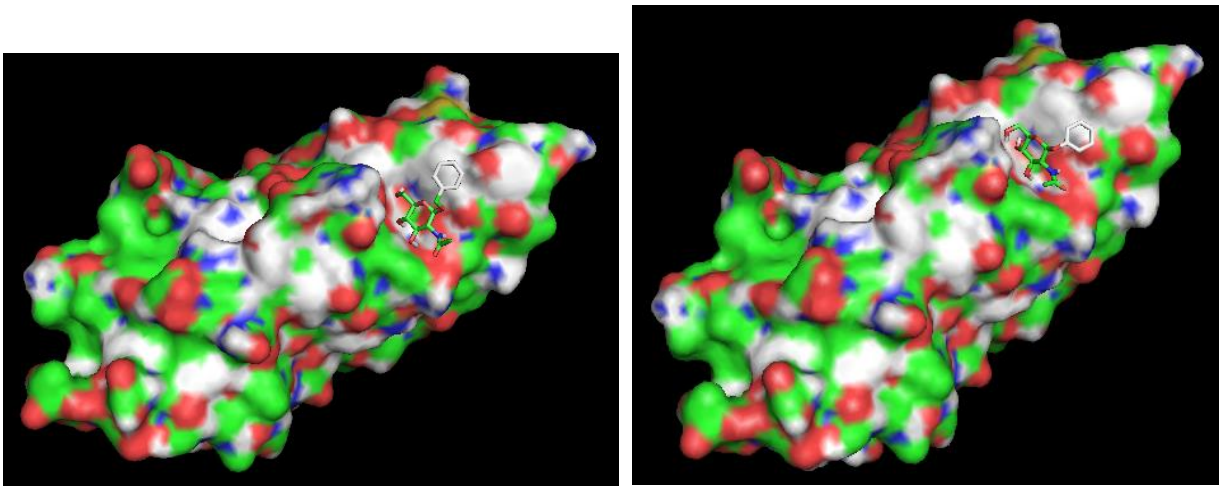

Figure 10. F17G protein surface complexed with benzyl glycoside (left) and phenyl glycoside (right)

There are several consistencies across the different glycoside docking studies, such as the tendency for hydrogen bonding between the carbon one oxygen and Ser116. This is observed in the top two poses for the benzyl and hexyl glycosides, and in the third pose for the phenyl glycoside. Hydrogen bonding between the amide hydrogen and Thr117 is observed in the top three poses of the phenyl, top two poses of hexyl, and top pose of the benzyl glycoside (Tables 6, 4, and 2). The hydrogen bonding with Thr117 and Ser116 are significant because they are consistent with the GlcNAc docking results reported here and previously investigated in the literature.[10] Likewise, Asp88 tends to form bidentate interactions with carbon four and carbon six. Despite disparities in binding affinities, the significant polar interactions are almost identical among the different glycosides and GlcNAc in pose one. This supports the idea that there are secondary interactions such as π stacking and solvent-shielding occurring between the glycosides and poses that contribute to variations in affinity and should be further investigated. One point of interest is at the first two poses of the hexyl docking, which give similar affinity measurements yet show the alkyl chain positioned in opposite directions (Figure 6). The first two carbons of the chain appear to be in the same position in both poses. This may indicate a CH-π stacking interaction between the chain and the aromatic Trp109 residue. In pose 2 the chain turns

inward towards the supposed hydrophobic region formed near Trp109. However, in pose 1 the chain flips in the opposite direction of the hydrophobic region and gives a higher affinity value. This may again be explained by CH-π stacking interaction between the alkyl chain and the nearby Tyr114 residue which can be seen in figure 4.

Overall, the docking results highlight the benzyl glycoside as the best potential inhibitor with the highest binding affinity. The lack of a considerable difference in affinity between the hexyl glycoside and the natural GlcNAc ligand binding affinities compared to the results of the aromatic glycosides emphasizes the importance of including an aromatic substituent in the development of high affinity inhibitors of *E. coli* adhesion. Future structure-activity-relationship (SAR) studies may involve derivatizing the benzyl substituent with electron donating groups, such as alkyl chains, and electron withdrawing groups, such as hydroxyls, to inquire what might further improve binding affinity. An aromatic glycoside with a alkyl and hydroxyl substituents may be advantageous due to the combination of CH-π stacking and hydrogen bonding with the previously mentioned nearby Tyr114 residue.

### 4.4 Future Work

Once the sugar library is fully prepared, purified, and characterized the sugar derivatives will be applied in ELISA-like assays to assess affinity and inhibition capacities compared to the natural GlcNAc ligand (Figure 10). In order to carry out the biological assays, *E.coli* bacteria will be cultured to express the lectin binding domains. Later, synthetic ligands will be tested for their ability to inhibit bacterial adhesion and biofilm formation using crystal violet and hemagglutination assays. *E. coli* strains lacking the lectin targets will be used as a control to identify any off-target effects. Furthermore, cell growth and death will be assessed in conjunction with the ligands to assure the goal of antivirulence rather than killing the bacteria. After effective ligands are identified, protein-ligand complexes will be crystallized and analyzed to elucidate binding interactions and provide insight for subsequent syntheses. Future work may involve investigations of similar bacterial proteins to maximize the application of the synthetic sugars developed in this work.

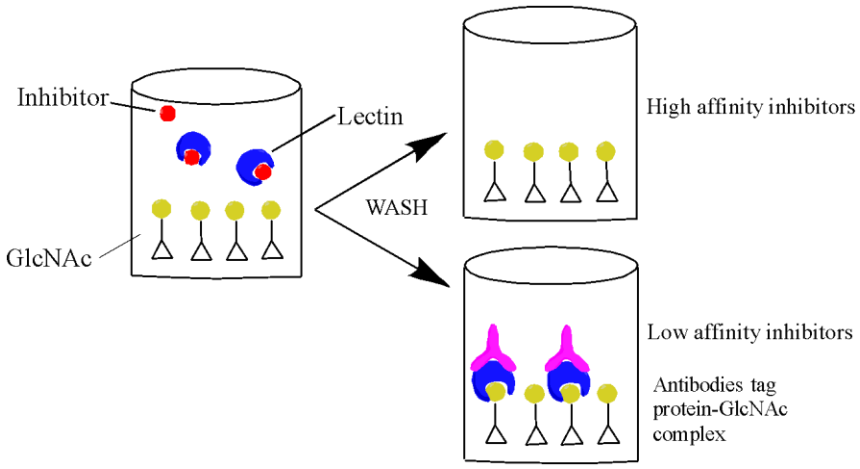


Figure 10. ELISA assay for assessing affinity of synthetic inhibitors versus natural GlcNAc ligand

## 5. Conclusion

Successful synthetic routes for benzyl, hexyl, and phenyl glycosides of GlcNAc have been established. Procedures involving GlcNAc chloride were found to be challenging and ineffective and were therefore disregarded. A glycosidation procedure using N-acetylglucosamine pentaacetate as the protected glycosyl acceptor and ytterbium triflate as an activator with benzyl alcohol, hexanol, and phenol were found to be effective for the purpose of this study. Purification of the deprotected benzyl and phenyl glycosides is in progress. The established procedures will allow for reliable synthesis of GlcNAc glycosides with varying characteristics. Thus, a small library of high affinity inhibitors will be developed for preventing *E. coli* adhesion and biofilm formation. Computational studies offer insight and better understanding of the binding interactions and generally show improved affinity of the glycosides as compared to the natural GlcNAc ligand. The benzyl glycoside shows the highest affinity for the F17G protein and is therefore the best potential inhibitor of *E.coli* adhesion according to this study. The phenyl glycoside had a slightly

lower affinity than the benzyl, and the hexyl glycoside was not a substantial improvement to the affinity of GlcNAc binding. Bacteria can express many different adhesins, and therefore this research complements the work that has been accomplished in developing mannose derivatives for FimH inhibition. The F17G and GafD fimbrial proteins play important roles in adhesion and fimbrial biogenesis, and therefore understanding the mechanisms by which they interact with a host is of utmost importance in antivirulence research.[15] This research continues to expand antivirulence knowledge for inhibition of *E.coli* adhesion and biofilm formation.

## 6. Acknowledgements

Special thanks to Dr. Caitlin McMahon for her support and guidance throughout this project, and to the UNC Asheville Department of Chemistry and Biochemistry for providing the space and resources needed to carry out this novel research.

## 7. References

[1] Totsika, M. Benefits and Challenges of Antivirulence Antimicrobials at the Dawn of the Post-Antibiotic Era. Drug Delivery Letters **2016**, *6* (1), 30–37.

[2] Antibiotic / Antimicrobial Resistance | CDC. **2020**

[3] Dickey, S. W.; Cheung, G. Y. C.; Otto, M. Different Drugs for Bad Bugs: Antivirulence Strategies in the Age of Antibiotic Resistance. *Nature Reviews Drug Discovery* **2017**, *16* (7), 457–471.

[4] Sommer, R.; Joachim, I.; Wagner, S.; Titz, A. New Approaches to Control Infections: Anti-Biofilm Strategies against Gram-Negative Bacteria. *CHIMIA International Journal for Chemistry* **2013**, *67* (4), 286–290.

[5] Muhsin J. et. al., Bacterial biofilm and associated infections. *Journal of the Chinese Medical Association*, **2018**, *81* (1), 7-11.

[6] Gilboa-Garber, N. , Avichezer, D. and Garber, N. C. Bacterial Lectins: Properties, Structure, Effects, Function and Applications. *Glycosciences,* **2008**, 21.

[7] Sharon, N. Carbohydrates as Future Anti-Adhesion Drugs for Infectious Diseases. *Biochimica et Biophysica Acta (BBA)*, **2005**, *1760* (4), 527–537.

[8]Korea, C. , Ghigo, J. and Beloin, C., The sweet connection: Solving the riddle of multiple sugar-binding fimbrial adhesins in *Escherichia coli., Bioessays*, **2011**, *33*, 300-311.

[9] Bouckaert, J.; Berglund, J.; Schembri, M.; Genst, E. D.; Cools, L.; Wuhrer, M.; Hung, C.-S.; Pinkner, J.; Slättegård, R.; Zavialov, A.; et al. Receptor Binding Studies Disclose a Novel Class of High-Affinity Inhibitors of the Escherichia Coli FimH Adhesin. *Molecular Microbiology* **2004**, *55* (2), 441–455.

[10] Merckel, M. et. al., The Structural Basis of Receptor-binding by Escherichia coli Associated with Diarrhea and Septicemia. *J. Mol. Biol.* **2003**, *331*, 897–905

[11] Lindhorst, T.K. A bivalent glycopeptide to target two putative carbohydrate binding sites on FimH. *J. Org. Chem*. **2010**, *6*, 801–809

[12] Hartmann, M.; Lindhorst, T. K. The Bacterial Lectin FimH, a Target for Drug Discovery - Carbohydrate Inhibitors of Type 1 Fimbriae-Mediated Bacterial Adhesion. *European Journal of Organic Chemistry* **2011**, (20-21), 3583–3609.

[13] Imberty, A.; Al., E. A. E., Multivalent Glycoconjugates as Anti-Pathogenic Agents. *Chem. Soc. Rev*., **2013**, *42*, 4709.

[14] Buts, L.; Bouckaert, J.; Genst, E. D.; Loris, R.; Oscarson, S.; Lahmann, M.; Messens, J.; Brosens, E.; Wyns, L.; Greve, H. D. The Fimbrial Adhesin F17-G of Enterotoxigenic *Escherichia Coli* Has an Immunoglobulin-like Lectin Domain That Binds N-Acetylglucosamine. *Molecular Microbiology* **2004**, *49* (3), 705–715.

[15] Saarela et. al., The Escherichia coli G-Fimbrial Lectin Protein Participates Both in Fimbrial Biogenesis and in Recognition of the Receptor N-Acetyl-D-Glucosamine. *Journal of Bacteriology*, **1955**, *177* (6), 1477-1484.

[16] Horton, D.; 2-acetamido-3,4,6-triacetyl-2-deoxy-α-D-glucopyranosyl chloride. *Org. Synth.* **1966,** 46, 1.

[17] B. R. Baker, J. P. Joseph, R. E. Schaub, and J. H. Williams, *J. Org. Chem.*, **1954,** *19* (11), 1717-1723

[18] Shultz, et. al. Chemoenzymatic Synthesis of 4-Fluoro-N-Acetylhexosamine Uridine Diphosphate Donors: Chain Terminators in Glycosaminoglycan Synthesis *J. Org. Chem.* **2017***, 82*, 2243−2248

[19] Difrancesco, B. R., Morrison, Z. A., & Nitz, M. Monosaccharide inhibitors targeting carbohydrate esterase family 4 de-N-acetylases. *Bioorg. & Med. Chem*. **2018**, *26* (21), 5631-5643

[20] Zemplen, G., Kuntz, A., *Ber*., **1924**, (57B), 1357

[21] Ye Cai, CCL., Bundle, D., Facile Approach to 2-Acetamido-2-deoxy-β-d-Glucopyranosides via a Furanosyl Oxazoline *Org. Lett.* **2005**, *7* (18), 4021–4024.

[22] Mukhopadhyay, B., Mandal, S., & Sharma, N., $H_2SO_4$-Silica Promoted Direct Formation of β-Glycosides of N-Acetyl Glycosylamines under Microwave Conditions. *Synlett*, **2009**, *19*, 3111–3114.

[23] Chupakhina, T., Kur'yanov, V., Chirva, V., Grigorash, R., Kotlyar, S., Kamalov, G., Aromatic Crown Ethers as Phase Transfer Catalysts in the Synthesis of N-Acetylglucosamine b-Aryl Glycosides. *Russian Journal of Bioorganic Chemistry* **2004**, 30 (3), 301–303

[23] Forli et. al. Computational protein-ligand docking and virtual drug screening with the AutoDock suite. *Nat Protoc*. **2016**, *11*(5), 905–919.

[24] Beau, J.M. et. al., Glycosylation: The Direct Synthesis of 2-Acetamido-2-Deoxy Sugar Glycosides *Eur. J. Org. Chem*. **2018**, 5795–5814